Technical Progress Report – EMSP 73914 (Renewal of 55164)

Reporting Period: 14 March 2001 – 14 November 2002

Submission Data: December 6, 2002

Agreement Number: DE-FG07-96ER62321

Title: Reductive immobilization of U(VI) in Fe(III) oxide-reducing subsurface sediments: Analysis of coupled microbial-geochemical processes in experimental reactive transport systems

Investigators: Eric E. Roden (PI)
Matilde M. Urrutia (Co-PI)
The University of Alabama
Department of Biological Sciences
Tuscaloosa, AL 35487-0206

Mark O. Barnett (Co-PI)
Clifford R. Lange (Co-PI)
Department of Civil Engineering
Auburn University
Auburn, AL 36849-5337

1. Research Objective

Although the fundamental microbiological and geochemical processes underlying the potential use of dissimilatory metal-reducing bacteria (DMRB) to create subsurface redox barriers for immobilization of uranium and other redox-sensitive metal/radionuclide contaminants are well-understood (Lovley et al., 1991; Gorby and Lovley, 1992; Lovley and Phillips, 1992; Lovley, 1995; Fredrickson et al., 2000; Wielinga et al., 2000; Wielinga et al., 2001), several fundamental scientific questions need to be addressed in order to understand and predict how such treatment procedures would function under *in situ* conditions in the subsurface. These questions revolve around the dynamic interactions between hydrologic flux and the coupled microbial-geochemical processes which are likely to occur within a redox barrier treatment zone. A brief summary of such questions includes the following:

A. *What are the kinetic limitations to the efficiency of microbial U(VI) scavenging in subsurface sediments?*

B. *Is U(VI) sorbed to Fe(III) oxide and other solid-phase surfaces subject to enzymatic reduction? If so, what are the relative kinetics of aqueous vs. sorbed U(VI) reduction?*

C. *What are the relative kinetics of direct, enzymatic U(VI) reduction vs. abiotic reduction of U(VI) by surface-bound biogenic Fe(II)?*

D. *Can coupled Fe(III) oxide/U(VI) reduction be sustained long-term in subsurface environments? What are the kinetic relationships between Fe(III) oxide reduction, DMRB growth, and U(VI) reduction in advectively open sedimentary systems?*

The overall objective of our research is to address the questions listed above through laboratory-based batch and reactive transport experiments with natural Fe(III) oxide-bearing subsurface materials and a representative pure culture DMRB. A unique feature of our research is that we are using levels of total uranium (ca. 10^{-6} to 10^{-4} mol per dm^3 bulk volume) and aqueous/solid-phase ratios ($\leq$ ca. 10^{-3} mol U per kg sediment) which are much closer to those present in contaminated subsurface environments compared to levels employed in previous experimental studies of microbial U(VI) reduction. The goal is to develop a more realistic picture of the dynamics of U(VI) reduction and its interaction with Fe(III) oxide reduction in subsurface sedimentary environments. In doing so, our studies will provide benchmark information on process dynamics that will be useful for scaling up (e.g. through the use of field-scale reactive transport models) to *in situ* treatment scenarios. In addition, the experimental methodologies and modeling strategies developed for the project may applicable to the evaluation of *in situ* remediation technologies for other redox-sensitive metal-radionuclide contaminants such as Cr(VI) and Tc(VII). Numerical simulations are being developed hand-in-hand with the experimental work to aid in the interpretation of the observed dynamics of U(VI) behavior, and to contribute to the development of a predictive framework for assessing *in situ* metal-radionuclide remediation strategies driven by the activity of DMRB.

2. Research Progress and Implications

This report summarizes ca. 1.5 years of research on a 3-year renewal of our original EMSP 96-10 project. Delays were encountered during recruitment and hiring of postdoctoral research associates at both UA and Auburn, such that these investigators did not begin work on the project until June 2002. Hence, we are somewhat behind schedule in relation to the timeline outlined in the research proposal. However, we have made good progress on the Phase I microbiological and geochemical studies, and have begun producing manuscripts for publication of this work. Work on the Phase II and Phase III components of the project will begin in January 2003.

Phase I Microbiological Studies – Kinetics Experiments in Batch Cultures

Overview of Research Methodology

Aqueous phase. The aqueous phase employed in our batch experiments is a Pipes-Buffered (10 mM, pH 6.8) Artificial Ground Water (PBAGW) containing ca. 10 mM dissolved inorganic carbon concentration (added as $NaHCO_3$) . The major ion composition of the PBAGW is similar to that formulated by DeFlaun et al. (1999) to model the groundwater at the DOE-NABIR bacterial transport research site in Oyster, VA, and to that employed in previous batch and column Fe(III) oxide reduction experiments in our laboratory (Roden et al., 2000; Roden, 2002). Sulfate was omitted from the AGW in order to prevent the activity of sulfate-reducing bacteria, whose spores could potentially survive autoclaving. Inorganic nutrient (10 μM KH_2PO_4, 100 μM NH_4Cl) concentrations are ca. 1000-fold lower than those typically included in anaerobic growth medium for Fe(III)-reducing bacteria (Lovley and Phillips, 1988). Small quantities of acid (HCl) or base (NaOH) are added to suspensions of solids as needed to achieve a starting pH of 6.8. The standard concentration of U(VI) used in experiments on enzymatic U(VI) reduction was 100 μM (added as uranyl-acetate). Lower concentrations (1 mg L^{-1} = 4.2 μM, added as uranyl-nitrate) were typically employed in U(VI) sorption experiments (see below).

Solid Phase. The majority of experiments to date have been conducted with iron-rich subsurface sands from the Abbott's Pit collection site in Mappsville, VA. The Abbott's Pit Sand (APS) is a reference material for the DOE NABIR program, and is representative of Fe(III) oxide-rich subsurface materials on DOE lands. The mineralogy of APS is comparable to that of other subsurface materials in the vicinity of the Oyster research site on the Delmarva Peninsula (Zachara et al., 1989). The Fe(III) oxide pool is dominated by crystalline goethite and feroxyhite (Zachara et al., 1989), with smaller quantities (ca. 10% of citrate dithionite-extractable Fe) of poorly crystalline Fe(III) oxides, as determined by short-term (1 hr) dilute (0.5M) HCl extraction. The APS material was wet-sieved through a 100 μm sieve and freeze-dried prior to being used in bacterial Fe(III) oxide reduction experiments. The sieving procedure was required to remove large sand grains which otherwise prevented sampling of batch reactors with our standard syringe-and-needle procedure. The <100 μm fraction of the subsurface material contained ca. 90% of the total citrate-dithionite extractable Fe. In most experiments, the sieved APS material was added to achieve a final Fe(III) oxide concentration of 50 mmol L^{-1}, which corresponded to ca. 88 g of solids per dm^3 of culture medium. This amount of solid in medium containing 100 μM U(VI) yields a mass-normalized U(VI) concentration of ca. 1 μmol per g of dry sediment, which is comparable to levels of total uranium in typical DOE-contaminated subsurface sediments (e.g. those at ORNL; (Watson, 2002)) Additional Fe(III)/U(VI) experiments were conducted with synthetic goethite, hematite, and ferrihydrite, prepared (or purchased) as described in previous research in our laboratory (Roden and Zachara, 1996; Roden, 2002).

Microorganism. The acetate-oxidizing, Fe(III)/U(VI)-reducing bacterium, *Geobacter sulfurreducens* (Caccavo et al., 1994) was employed in all of the Fe(III) and U(VI) reduction experiments described herein. This organism is the subject of several DOE NABIR research projects (directed by D. Lovley, University of Massachusetts and J. Lloyd, University of Manchester) on the biochemistry and genetics of Fe(III), U(VI) and Tc(VII) reduction. Hence it is logical to compile information on the performance of this organism in experimental studies of the biogeochemistry of metal-radionuclide contaminant reduction. In addition, the fact that the majority of Fe(III)-reducing organisms which arise during stimulation of Fe(III) oxide (and U(VI)) reduction activity in subsurface sediments (Snoeyenbos-West et al., 2000; Holmes et al., 2002) are closely related to *G. sulfurreducens* indicates that this is an appropriate model organism for experimental studies of subsurface metal reduction and associated biogeochemistry. *G. sulfurreducens* can be grown to a high cell density with malate (or fumarate) as an electron acceptor, and cells grown in this manner have a strong capacity for solid-phase Fe(III) oxide (Roden and Urrutia,

2002) and U(VI) reduction (Caccavo et al., 1994). Washed, malate-grown *G. sulfurreducens* cells therefore provided an ideal inoculum for our Fe(III) and U(VI) experiments.

Kinetics of Fe(III) oxide reduction and DMRB growth

A series of Fe(III) oxide reduction experiments was conducted in order to provide data required for quantitative simulation of bacterial Fe(III) oxide reduction activity in subsurface sediments. As observed in previous studies of solid-phase Fe(III) oxide reduction (Roden and Zachara, 1996; Roden and Urrutia, 1999), rates of APS Fe(III) oxide reduction (determined by monitoring rates of 0.5M HCl-extractable Fe(II) over time) were linearly related to Fe(III) oxide abundance (Fig. 1), and hyperbolically related to DMRB (*G. sulfurreducens*) cell abundance (Fig. 2). Based on the results of these experiments, we have assembled a model (see Appendix 1) of bacterial Fe(III) oxide reduction in which rates of Fe(III) reduction and DMRB growth are dependent on the abundance of both DMRB cells and available oxide surface sites, as modified by sorption of biogenic Fe(II) which is assumed to render surface sites unavailable for reduction (Roden and Urrutia, 1999). The model successfully reproduced the time course of Fe(III) reduction in experiments with different initial DMRB abundance. This model has been incorporated into a multiple pore region simulation of coupled Fe(III)/U(VI) reduction in fractured subsurface sediments (Roden and Scheibe, 2002). At present, we have not yet arrived at a standard procedure for measuring DMRB biomass in our reaction systems, so it has not yet been possible to verify predicted changes in DMRB abundance in the batch Fe(III) oxide reduction simulations (e.g. in runs where the initial biomass starts at a relatively low value of ca. 10^5 cells mL^{-1} and increase by 2-3 orders of magnitude during the simulation). However, we are making good progress in development of an ATP-based assay of DMRB cell abundance, which will eventually be used to verify predicted changes in DMRB biomass. In addition, we are continuing to evaluate the utility of a ^{3}H-leucine incorporation technique for estimation of instantaneous growth rates of DMRB coupled to Fe(III) oxide reduction.

Kinetics of aqueous U(VI) reduction by G. sulfurreducens

The kinetics of aqueous U(VI) reduction by *G. sulfurreducens* was determined in PBAGW containing 10 mM $NaHCO_3$, 10 mM acetate, and ca. 10^8 mL^{-1} of washed, acetate/fumarate-grown cells. Changes in aqueous U(VI) concentration were determined hourly over a 3-hr incubation period with a Kinetic Phosphorescence Analyzer (KPA; Chemchek Instruments, Richland, WA), and rates of U(VI) reduction were determined by linear regression analysis of the time course data. V_{max} and K_m values were estimated from nonlinear regression analysis of a plot of U(VI) reduction rate vs. initial U(VI) concentration (Fig. 3). The values obtained are comparable to those reported for other DMRB (Truex et al., 1997; Liu et al., 2002).

An important implication of the above findings is that they confirm that half-saturation constants for U(VI) reduction by known species of DMRB are 10-100 fold higher than typical aqueous U(VI) concentrations in contaminated subsurface sediments. Hence, rates of U(VI) reduction and growth DMRB coupled to U(VI) reduction will always be strongly limited by U(VI) availability, with the upshot that much of the growth of DMRB during subsurface reductive immobilization procedures is likely to be coupled to Fe(III) oxide reduction rather than reduction of U(VI) and other trace metal-radionuclide contaminants (Finneran et al., 2002). This fact emphasizes the need for development of a detailed mechanistic (and ultimately predictive) understanding of the controls on subsurface Fe(III) oxide reduction and associated DMRB growth.

Kinetics of sorbed U(VI) reduction

An extensive series of batch culture experiments has been conducted to examine the potential for enzymatic reduction of U(VI) associated with Fe(III) oxide surfaces. In these experiments, virtually all (> 95%) of the U(VI) was associated with the solid-phase, presumably through complexation of uranyl and uranyl-carbonate ions by Fe(III) oxide surfaces (e.g. (Waite et al., 1994; Barnett et al., 2002)). In order to monitor reduction of U(VI) in these systems, culture samples were extracted with 100 mM $NaHCO_3$ (pH 8.9) under anaerobic conditions, after which the amount of U(VI) in the extract was determined by KPA. For the sake of consistency, U(VI) reduction in parallel oxide-free cultures was monitored by the same procedure.

Figure 4 shows the results of three experiments examining U(VI) reduction in the presence and absence of APS material (50 mmol Fe(III) L^{-1}). The results show for the first time that U(VI) associated with natural Fe(III) oxide-bearing subsurface material is subject to enzymatic reduction (Fig. 4A). However, the rate and extent of sorbed U(VI) reduction was lower than that in medium lacking APS (compare Figs 4A and B). Rates of Fe(III) reduction were identical in the presence and absence of ca. 100 μmol L^{-1} total U(VI) (Figs. 4C and D), which indicates that DMRB activity was not compromised by the presence of U(VI). In contrast to results obtained with APS, experiments with cultures containing synthetic medium surface area (MSA) or high surface area (HSA) goethite (which had BET-determined specific surface areas of ca. 55 and 150 m^2g^{-1}, respectively; see Roden and Zachara (1996)) demonstrated nearly identical rates of U(VI) reduction in the presence and absence 50 mmol Fe(III) L^{-1} (Fig. 5).

We speculated that the reason for the incomplete reduction of sorbed U(VI) in APS-containing medium was that some of the U(VI) became associated with particle surfaces that were inaccessible to the outer membrane reductases (sensu Lovley (2000)) of *G. sulfurreducens*. Although we can rule out slow diffusion of U(VI) into progressively smaller pore size classes based on time course studies of U(VI) adsorption (see below), the possibility nevertheless exists that some fraction of sites occupied by sorbed U(VI) were, for as yet undefined physical and/or steric reasons, unavailable to the DMRB reductases. In order to evaluate this hypothesis, we conducted an experiment in which a catalytic amount (100 μM) of the electron shuttling compound AQDS was either added to the culture system at the start of the experiment, or added after U(VI) reduction had leveled-off at ca. 50% as observed in other experiments. AQDS is a small (<1 kD) synthetic quinone compound which has been used as an analog to the quinone moieties of natural humic substances (Lovley et al., 1996). AQDS is subject to enzymatic reduction by DMRB, and in its reduced form (AHDS) is capable of shuttling electrons to solid-phase Fe(III) oxides, thereby accelerating rates of oxide reduction (Lovley et al., 1996; Lovley et al., 1998; Fredrickson et al., 1999). In addition, AHDS can transfer electrons to U(VI), and thereby increase rates of enzymatic U(VI) reduction (Fredrickson et al., 2000). We reasoned that the presence of AQDS in our batch Fe(III)/U(VI) reduction cultures would increase both the rate and extent of U(VI) reduction, by (i) speeding up the total rate of electron transfer, and (ii) by entering pore spaces that are inaccessible to the DMRB enzymatic system. The results of the experiment confirmed these expectations (Fig. 6): U(VI) and Fe(III) oxide reduction occurred much more rapidly in cultures amended with AQDS at the start of the experiment. Moreover, addition of 100 μM AQDS after U(VI) reduction had leveled off in cultures which did not initially contain AQDS led to rapid decline in U(VI) and a parallel stimulation of Fe(III) oxide reduction. As discussed below, we have no evidence that Fe(II) generated during bacterial Fe(III) oxide reduction is capable of promoting abiotic U(VI) reduction under the conditions used in our experiments. Hence, the observed stimulation of U(VI) reduction by the presence of AQDS cannot be attributed to a greater abundance of biogenic Fe(II). Rather, it is likely that the enhanced reduction of sorbed U(VI) and solid-phase Fe(III) were both stimulated by the ability of AHDS to contact oxide surface sites that were otherwise inaccessible to the DMRB.

We are in the process of obtaining Fe(III)-oxide bearing subsurface materials from other DOE sites (Oak Ridge, Hanford, and Savannah River), and will conduct analogous experiments with these materials within the next few months. If the results of these experiments are consistent with those obtained with APS, the findings will have important implications for understanding the potential for enzymatic reduction of U(VI) sorbed to natural subsurface sediments. As explained in the project proposal, reduction of sorbed U(VI) could dramatically enhance the efficiency of U(VI) scavenging in subsurface redox barrier environments, since bulk sediment concentrations of U(VI) are likely to be 10-100 fold higher than aqueous-phase concentrations. In addition, this process could help to immobilize large quantities of U(VI) *at their source* in vicinity of locations where U(VI) was originally introduced into the soil/groundwater system, thereby reducing the size of the treatment zone required to prevent off-site migration of U(VI). Development of a better mechanistic understanding of the controls on enzymatic reduction of sorbed U(VI), as well as an appropriate quantitative framework for incorporation of this process into numerical simulation of U(VI) reactive transport in the subsurface, represents an important goal of this project.

Phase I Geochemical Studies – Batch Sorption and Abiotic U(VI) Reduction

Batch U(VI) sorption on Fe(III) oxide-bearing materials

The kinetics and equilibrium adsorption of U(VI) to a synthetic Fe(III) oxide-coated sand and unsieved APS were conducted in PBAGW containing 10 mM $NaHCO_3$ (Figs. 7-9), and in other background inorganic matrices (data not shown). The kinetics of U(VI) adsorption to both solid materials is shown in Fig. 7. These results indicate that U(VI) adsorbs more strongly to the APS sediment than the Fe-coated sand under the conditions of equivalent mass loading, which is consistent with the higher Fe content of the APS material. These results also indicate that the rate of U(VI) uptake by these materials is relatively rapid: aqueous concentrations after one hour were not significantly ($P<0.05$) different than concentrations after 2 days. Similar results were obtained in longer term (28 day) experiments (data not shown). These results indicate that U(VI) reaches equilibrium with these two materials over a relatively short time span (<2 hours), and that slow diffusion of U(VI) into interior particle porosity is not an important process. Additional experimentation showed that variations in dissolved inorganic carbon concentration from 2 to 10 mM did not strongly affect the rate of U(VI) sorption to these media.

Isotherms for U(VI) adsorption onto the two Fe(III) oxide-bearing materials are shown in Fig. 8. The results indicate that U(VI) adsorption is linear up to a dry weight-normalized total U(VI) content (1-2 $\mu mol\ g^{-1}$) comparable to that employed in the coupled Fe(III)/U(VI) reduction experiments described above. The combination of linear adsorption and the attainment of relatively rapid adsorption equilibrium indicate that relatively simple transport models (i.e. ones which assume linear local equilibrium) have the potential to accurately describe subsurface U(VI) transport. However, as previously reported for other synthetic (Hsi and Langmuir, 1985; Waite et al., 1994; Morrison et al., 1995; Kohler et al., 1996) and natural (Casas et al., 1994; Ticknor, 1994; Barnett et al., 2002) Fe(III) oxide minerals, U(VI) adsorption to these two media is strongly pH-dependent (Fig. 9). The combination of rapid and linear, but pH-dependent, adsorption of U(VI) to these materials indicates that a simple non-electrostatic pH-dependent adsorption modeling approach has the potential to accurately describe U(VI) subsurface transport, and in particular the behavior of U(VI) in the experimental reactive transport experiments to be conducted in Phases II and III of this research project.

Abiotic reduction of U(VI) by Fe(II)

The potential for abiotic reduction of U(VI) by Fe(II) produced during bacterial Fe(III) oxide reduction is an important issue with regard to the development of subsurface redox barrier technology for *in situ* immobilization of redox-sensitive metal-radionuclide contaminants. If biogenic Fe(II), particularly Fe(II) associated with solid-phase minerals (e.g. layered silicates and/or residual Fe(III) oxide surfaces) is capable of promoting rapid abiotic contaminant reduction, then it should be possible to achieve effective remediation through only periodic stimulation of DMRB activity so as to renew the capacity of the sediment for Fe(II)-promoted contaminant reduction. Such a strategy is likely to be effective in the case of Cr(VI) remediation, since both aqueous and surface-bound Fe(II) produced during bacterial Fe(III) oxide reduction are excellent reductants for soluble CrO_4^{2-} ions (Wielinga et al., 2001). In contrast, the potential for Fe(II)-promoted abiotic reduction of U(VI) is less certain. Although there is clear evidence that this process can occur under specific conditions in laboratory systems (Liger et al., 1999; Fredrickson et al., 2000) other studies indicate that such abiotic pathways are not likely to be effective mechanisms for U(VI) reduction in subsurface sediments in comparison with direct microbial reduction (Finneran et al., 2002; Senko et al., 2002).

We have evaluated the potential for abiotic reduction of U(VI) by Fe(II) in our experimental reaction systems in three ways. First, APS in anaerobic PBAGW was amended with an excess of Fe(II) (ca. 1 mmol L^{-1}, added from an anaerobic stock solution of $FeCl_2 \cdot 2H_2O$), after which ca. 100 μM U(VI) was added and the concentration of total U(VI) was monitored over time in comparison with systems to which no Fe(II) was added. Greater than 95% of the added Fe(II) and U(VI) were associated with the solid-phase at the start of these experiments. The results indicate that the solid-phase Fe(II) was not capable of transferring electrons to the sorbed U(VI) (Fig. 10). Although the reason for the decline in total U(VI) (Fig. 10A) and Fe(II) (Fig. 10B) over time in the reaction systems is unclear, the important point is that the presence of Fe(II) did not accelerate U(VI) loss, nor did the presence of U(VI) promote loss of Fe(II).

Second, microbially-reduced APS that had never been exposed to U(VI) (the "U(VI)-free controls" from coupled Fe(III)/U(VI) reduction experiments with *G. sulfurreducens*) was pasteurized, and then spiked with with 100 μM U(VI). No significant reduction of U(VI) or loss of Fe(II) was observed over a 2-week time period (Fig. 11).

Finally, we conducted an experiment in which APS reduction was allowed to proceed for 5 days, after which half of the cultures were killed by pasteurization. The cultures were amended with 100 μM U(VI), and the concentration of total U(VI) was monitored over time in live vs. killed systems. The results showed that substantial U(VI) reduction took place in the live cultures, whereas no significant loss of U(VI) occurred in the killed systems (Fig. 12A). The presence of ongoing metal-reduction activity in the live cultures was verified by the continued production of Fe(II) (Fig. 12B).

Taken together, our results provide substantial evidence *against* the potential for abiotic U(VI) reduction by Fe(II) produced in circumneutral Fe(III) oxide-reducing environments. Additional experiments are planned to evaluate the influence of pH on the kinetics of abiotic U(VI) reduction by surface-bound Fe(II) (Liger et al., 1999) in our reaction systems. If the lack of significant Fe(II)-promoted U(VI) reduction suggested by our initial experiments proves to be a robust result, the major implication for development of subsurface U(VI) reductive immobilization strategies is that active DMRB metabolism will need to be sustained in order to maintain ongoing U(VI) reduction activity. This will require the continual presence of electron donor and electron-accepting conditions sufficient to permit maintenance of significant populations of active DMRB. The experimental and modeling studies of bacterial Fe(III) oxide reduction and DMRB growth being conducted as part of this research project are likely to prove useful in

development of long-term U(VI) remediation scenarios based on biological (i.e. enzymatic) reduction pathways.

3. Planned Activities

Now that have developed (through the Phase I research summarized above) a working understanding of batch Fe(III)/U(VI) reduction systems (including U(VI) surface complexation), the next step will be to evaluate the potential for sustained U(VI) reduction in experimental reactive transport systems. As described in the project work plan, semicontinuous cultures (Phase II microbiological) and flow-through column reactors (Phase II geochemical, Phase III microbiological and geochemical) will be employed to address this question. We have extensive experience in the use of the semicontinuous and column reactors derived from previous EMSP-funded research. We recently verified our ability to pack replicate column reactors (10 cm long, 1 cm diameter) so as to achieve relatively uniform hydraulic properties. Parallel flow-through column U(VI) sorption experiments will be conducted at Auburn University with a variety of Fe(III) oxide-bearing materials in order to verify the ability of surface complexation models to accurately depict U(VI) sorption in a reactive transport setting. Further development of mixed kinetic/equilibrium simulations of U(VI) reactive transport in Fe(III) oxide-reducing will be pursued in parallel with the experimental studies.

4. Information Access

Referred Publications Supported by the Project

Roden, E.E. and M.M. Urrutia. 2002. Influence of biogenic Fe(II) on bacterial crystalline Fe(III) oxide reduction. *Geomicrobiol. J.* 19:209-251.*

Roden, E.E. and R.G. Wetzel. 2002. Kinetics of microbial Fe(III) oxide reduction in freshwater wetland sediments. *Limnol. Oceanogr*. 47:198-211.*

Barnett, M.O., P.M. Jardine, S.C. Brooks. 2002. U(VI) adsorption to heterogeneous media: application of a surface complexation model. *Environ. Sci. Technol.* 36:937-942.†

Roden, E.E., M.R. Leonardo, and F.G. Ferris. 2002. Immobilization of strontium during iron biomineralization coupled to dissimilatory hydrous ferric oxide reduction. *Geochim. Cosmochim. Acta* 66:2823-2839.*

* PDFs of these papers available at:
http://bama.ua.edu/~eroden/Publications/ListofPublications.htm

† PDF available at:
http://bama.ua.edu/~eroden/EMSPUVIFeIIIRedProject/EMSPUVIFeIIIRedProjectPublications.htm

Submitted Manuscripts

Roden, E.E. Heterogeneity of Fe(III) oxide reactivity with respect to biotic vs. abiotic reduction. *Environ. Sci. Technol.* Submitted for publication August 2002. (preprint available on request)

Roden, E.E. Diversion of electron flow from methanogenesis to crystalline Fe(III) oxide reduction in carbon-limited cultures of wetland sediment bacteria. *Appl. Environ. Microbiol*. Submitted for publication August 2002; in revision. (preprint available on request).

Roden, E.E. and T.D. Scheibe. Conceptual and numerical model of uranium(VI) reductive immobilization in structured subsurface media. *Environ. Sci. Technol*. (preprint available on request).

Manuscripts in Preparation

Roden, E.E., M.O. Barnett, and B.H. Jeon. A batch reaction model of coupled Fe(III)/U(VI) reduction in subsurface sediments.

Jeon, B.H., M.O. Barnett, and E.E. Roden. Enzymatic reduction of U(VI) associated with Fe(III) oxide surfaces.

Choi, J. and M.O. Barnett. Kinetic and equilibrium sorption of U(VI) to subsurface Fe(III) oxide phases.

Presentations at Scientific Conferences

Barnett, M.O., E.E. Roden, P.M. Jardine, S.C. Brooks. 2001. Biogeochemical interactions of U and Fe(III) oxides in subsurface environments: modeling and experimental results. American Chemical Society National Meeting, August 2001. PowerPoint presentation available at: http://bama.ua.edu/~eroden/EMSPUVIFeIIIRedProject/EMSPUVIFeIIIRedProjectIndex.htm

Roden, E.E. and M.O. Barnett. 2002. Reductive immobilization of U(VI) in Fe(III) oxide-reducing subsurface sediments. Poster at joint SCFA-DCFA meeting, March 2002

Roden, E.E. and T.D. Scheibe. 2002. Multiple pore region model of uranium(VI) reductive immobilization in structured subsurface media. American Geophysical Union Meeting, December 2002.

B.H. Jeon and E.E. Roden. 2003. Reductive immobilization of U(VI) at the oxide-water interface. American Chemical Society National Meeting, March 2003.

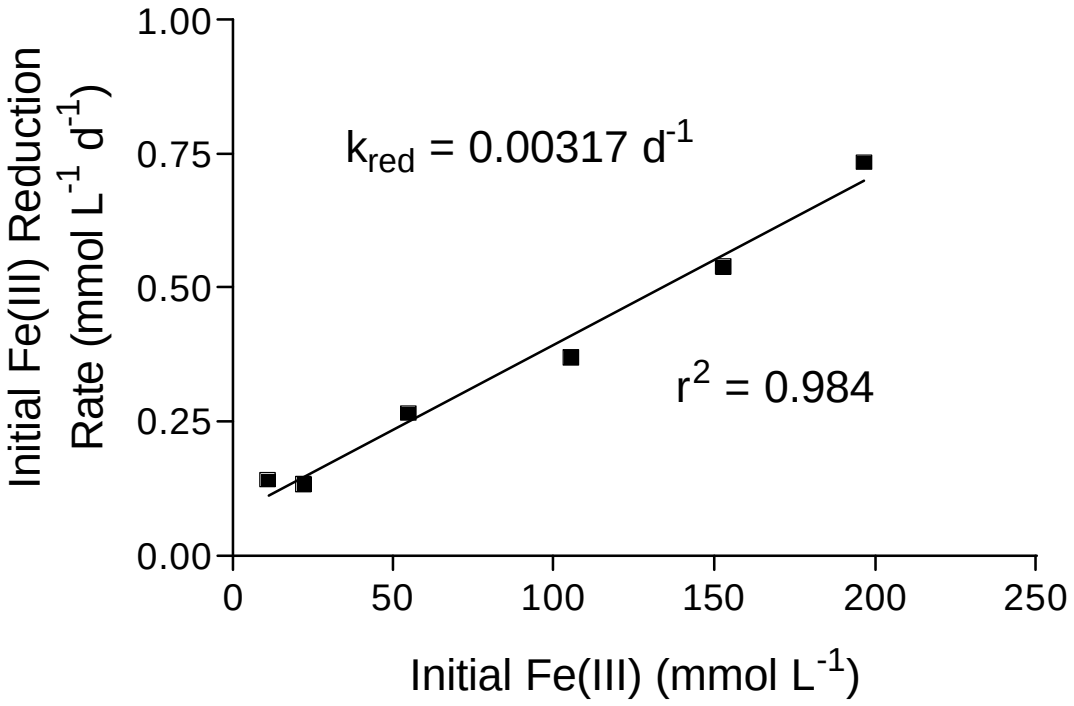

Figure 1. Initial rate of APS Fe(III) oxide reduction by *G. sulfurreducens* (10^8 cells mL^{-1}) under nongrowth conditions as a function of initial Fe(III) oxide abundance. Data points represent the means of duplicate cultures. The line shows a linear least-squares regression fit of the data.

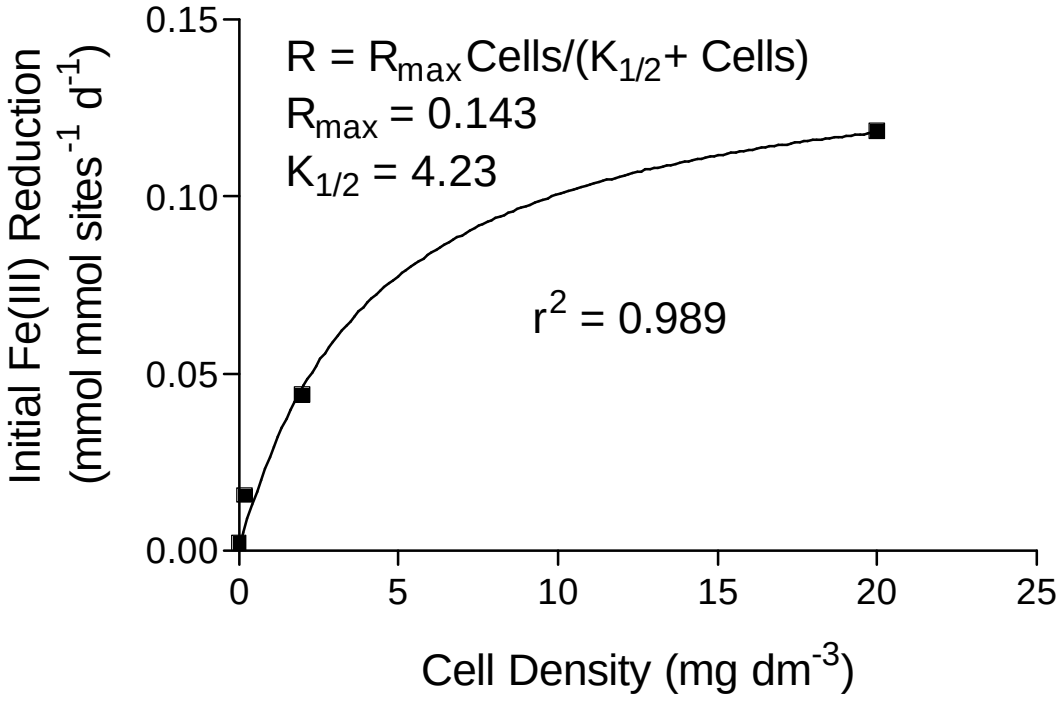

Figure 2. Initial rate of APS Fe(III) oxide reduction (Fe(III) = 40 mmol L^{-1}) by *G. sulfurreducens* under nongrowth conditions as a function of cell density. Data points represent the means of duplicate cultures. The density of oxide surface sites assumed in the calculation of reaction rates is explained in Appendix 1. The line shows a nonlinear least-squares regression fit of the data to a hyperbolic kinetic function. A cell density of 20 mg dm^{-3} corresponds to ca. 10^8 cells mL^{-1}.

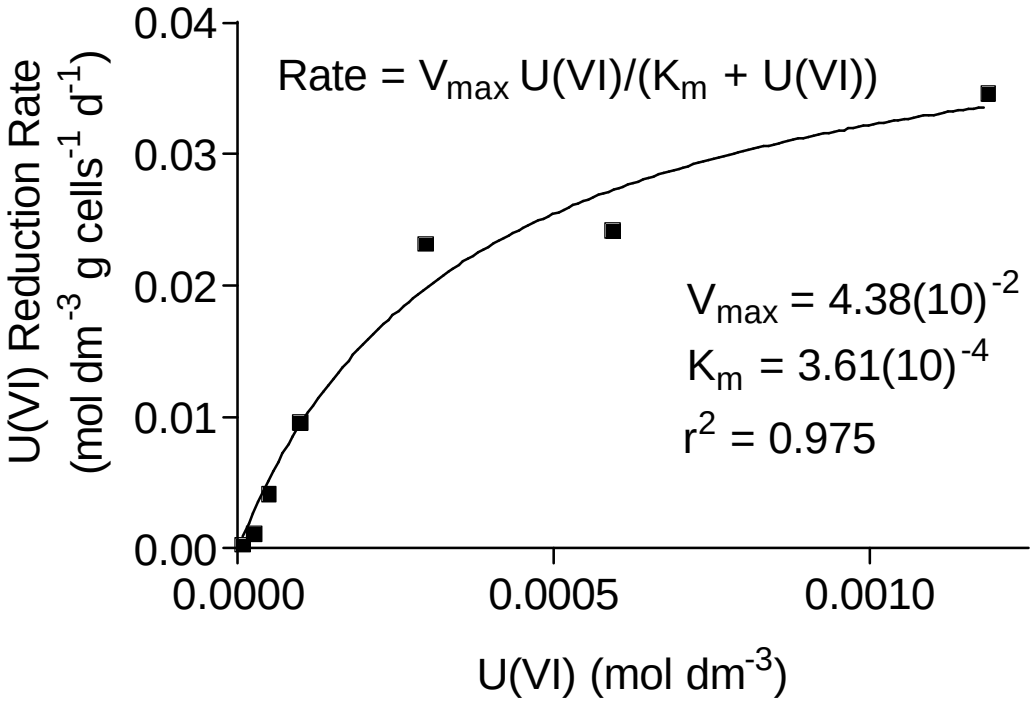

Figure 3. Kinetics of aqueous U(VI) reduction by *G. sulfurreducens* (10^8 cells mL^{-1}). Data points represent the means of triplicate cultures. The line shows a nonlinear least-squares regression fit of the data to a hyperbolic kinetic function.

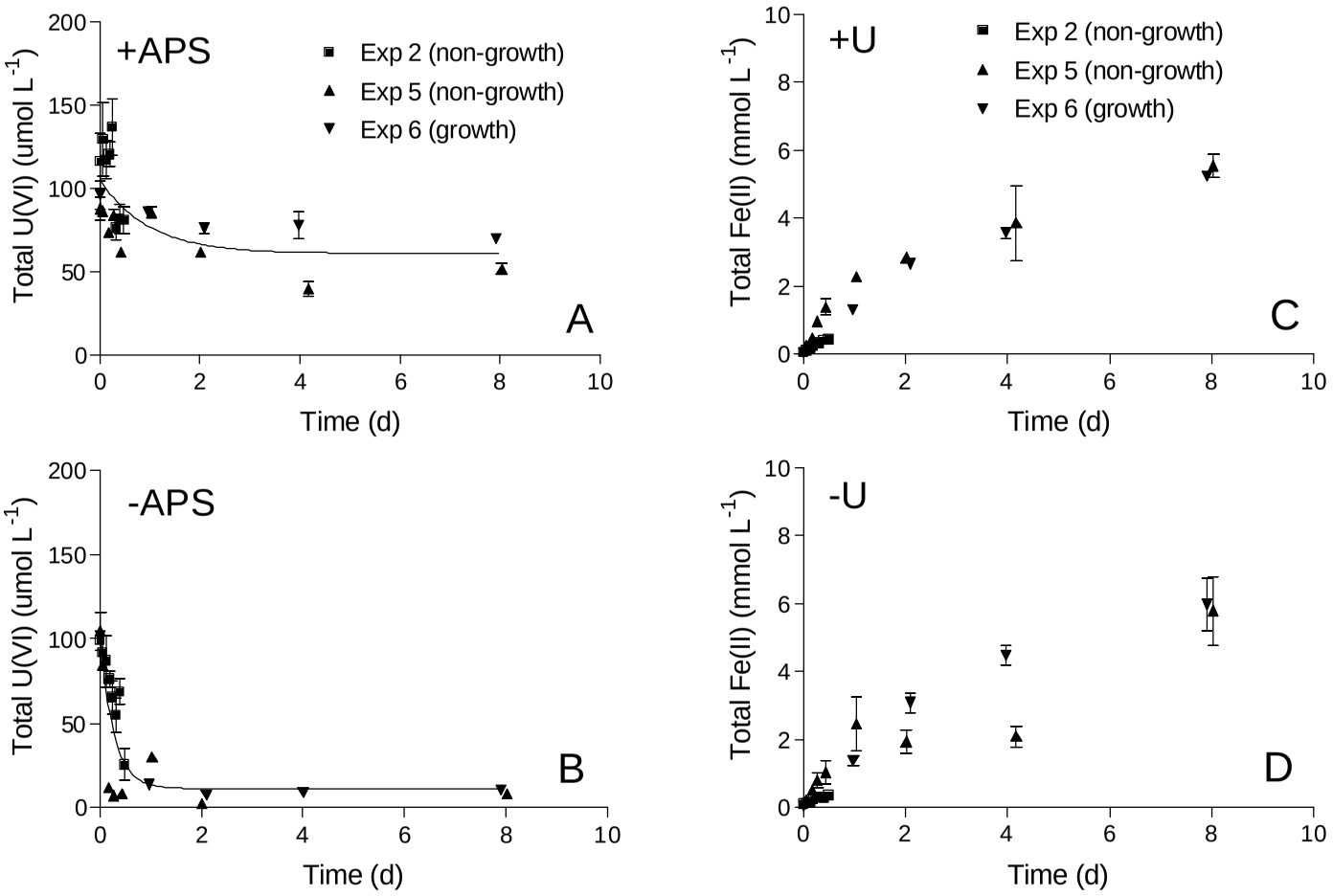

Figure 4. Reduction of U(VI) and Fe(III) by *G. sulfurreducens* (10^8 cells mL^{-1}) in the presence (A) or absence (B) of APS (50 mmol Fe(III) L^{-1}). Virtually all (> 95%) of the U(VI) in cultures containing APS was associated with the solid-phase at the start of the experiment. Panels C and D show rates of Fe(III) reduction in culture systems with and without 100 mM U(VI). Data points represent the means ± SD of triplicate cultures. Lines in panels A and B are nonlinear least-squares regression fits of the aggregated data to the following equation: $C(t) = (C_0 – C^*)\exp(-kt) + C^*$, where C_0 is the initial total U(VI) concentration, and C*is the asymptotic U(VI) concentration at the end of the experiment.

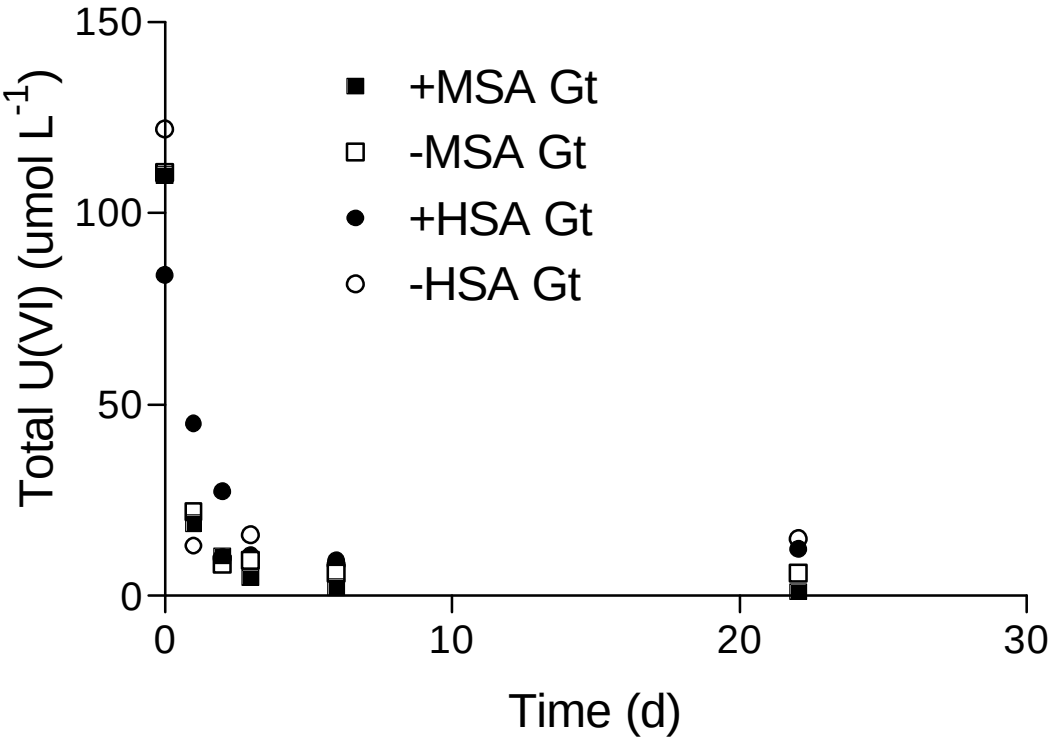

Figure 5. Reduction of U(VI) by *G. sulfurreducens* (10^8 cells mL^{-1}) in the presence or absence of 50 mmol L^{-1} of either synthetic medium surface area (MSA) goethite (55 m^2 g^{-1}) or high surface area (HSA) goethite (150 m^2 g^{-1}). Virtually all (> 95%) of the U(VI) in cultures containing synthetic goethite was associated with the solid-phase at the start of the experiment. Data points represent the means of duplicate cultures.

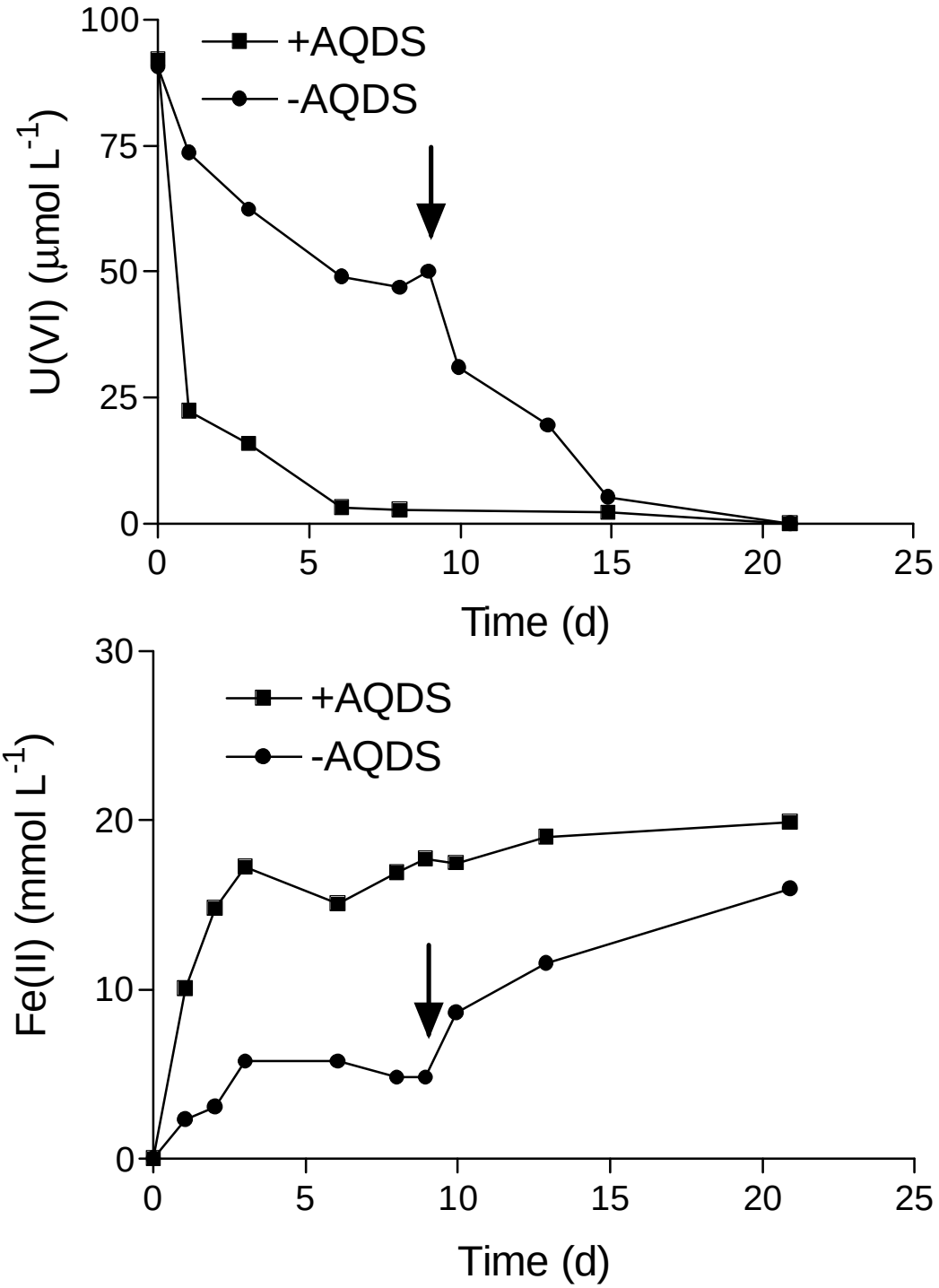

Figure 6. Reduction of U(VI) (A) and Fe(III) (B) by *G. sulfurreducens* (10^8 cells mL^{-1}) in APS-containing medium (50 mmol Fe(III) L^{-1}) with or without 100 mM AQDS at the start of the experiment. The arrows indicates time at which 100 mM AQDS was added to cultures which did not initially contain AQDS. Data points represent the means of triplicate cultures.

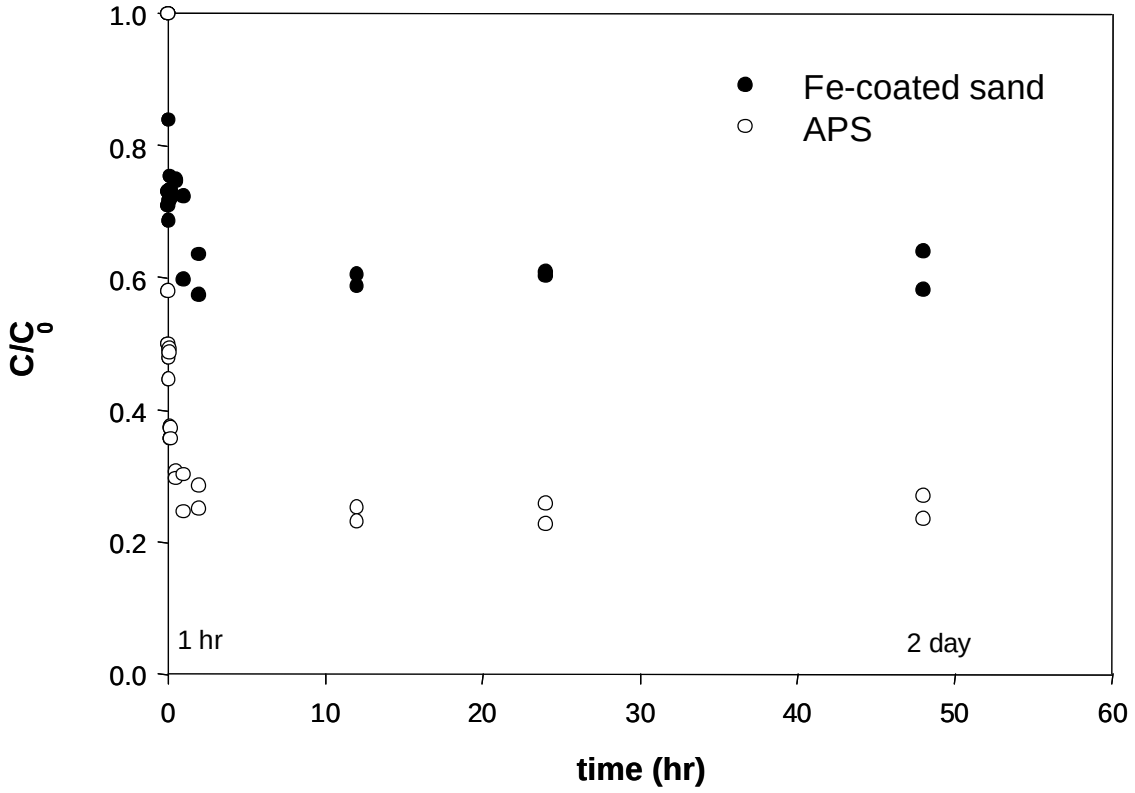

Figure 7. Kinetics of U(VI) (1 mg L^{-1}) sorption onto synthetic Fe(III) oxide-coated sand or APS (both at 16.7 g L^{-1}) in PBAGW containing 10 mM $NaHCO_3$. Data points show the results of duplicates.

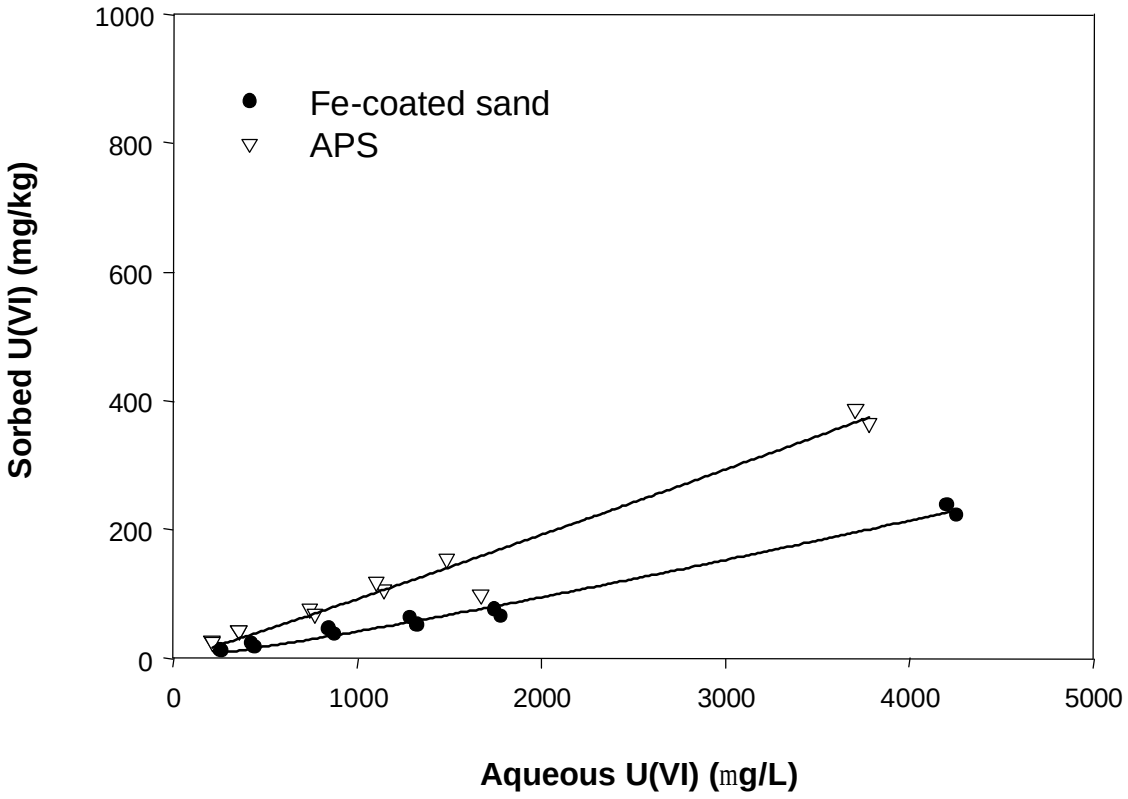

Figure 8. Isotherm for U(VI) sorption onto synthetic Fe(III) oxide-coated sand and APS material (both at 3.33 g L^{-1}) in PBAGW containing 10 mM $NaHCO_3$. Data points show the results of duplicates. Solid lines show linear least-squares regression fits of the data.

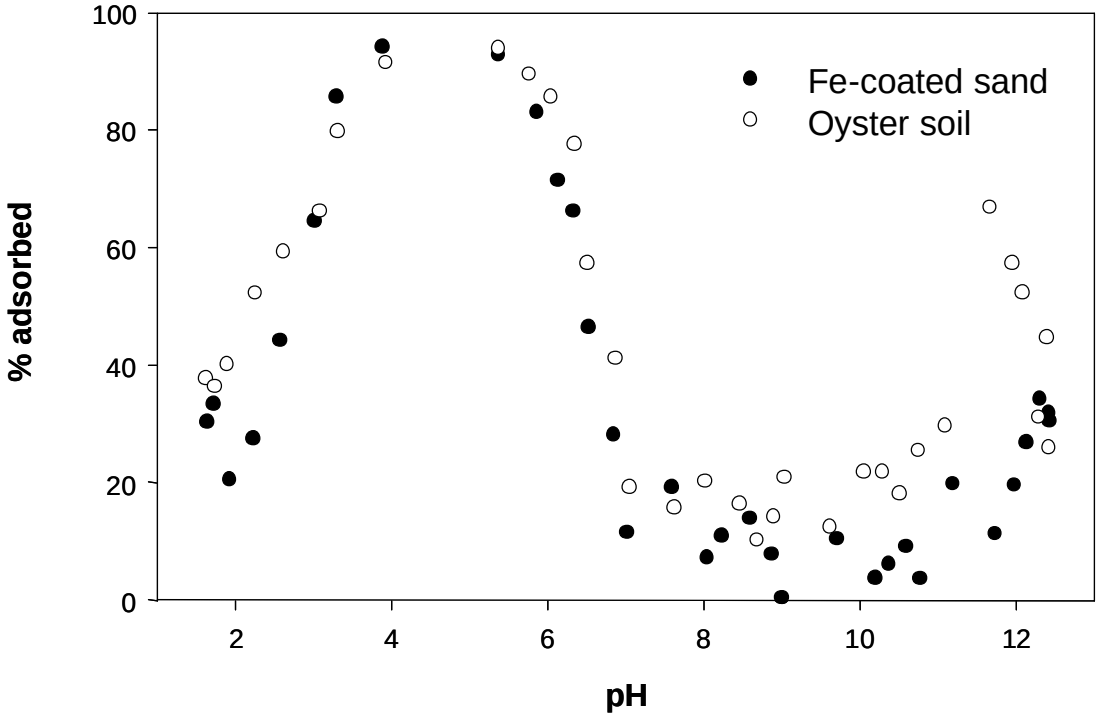

Figure 9. pH dependence of U(VI) (1 mg L^{-1}) sorption onto the synthetic Fe(III) oxide-coated sand and APS material (both at 3.33 g L^{-1}) in PBAGW containing 10 mM $NaHCO_3$.

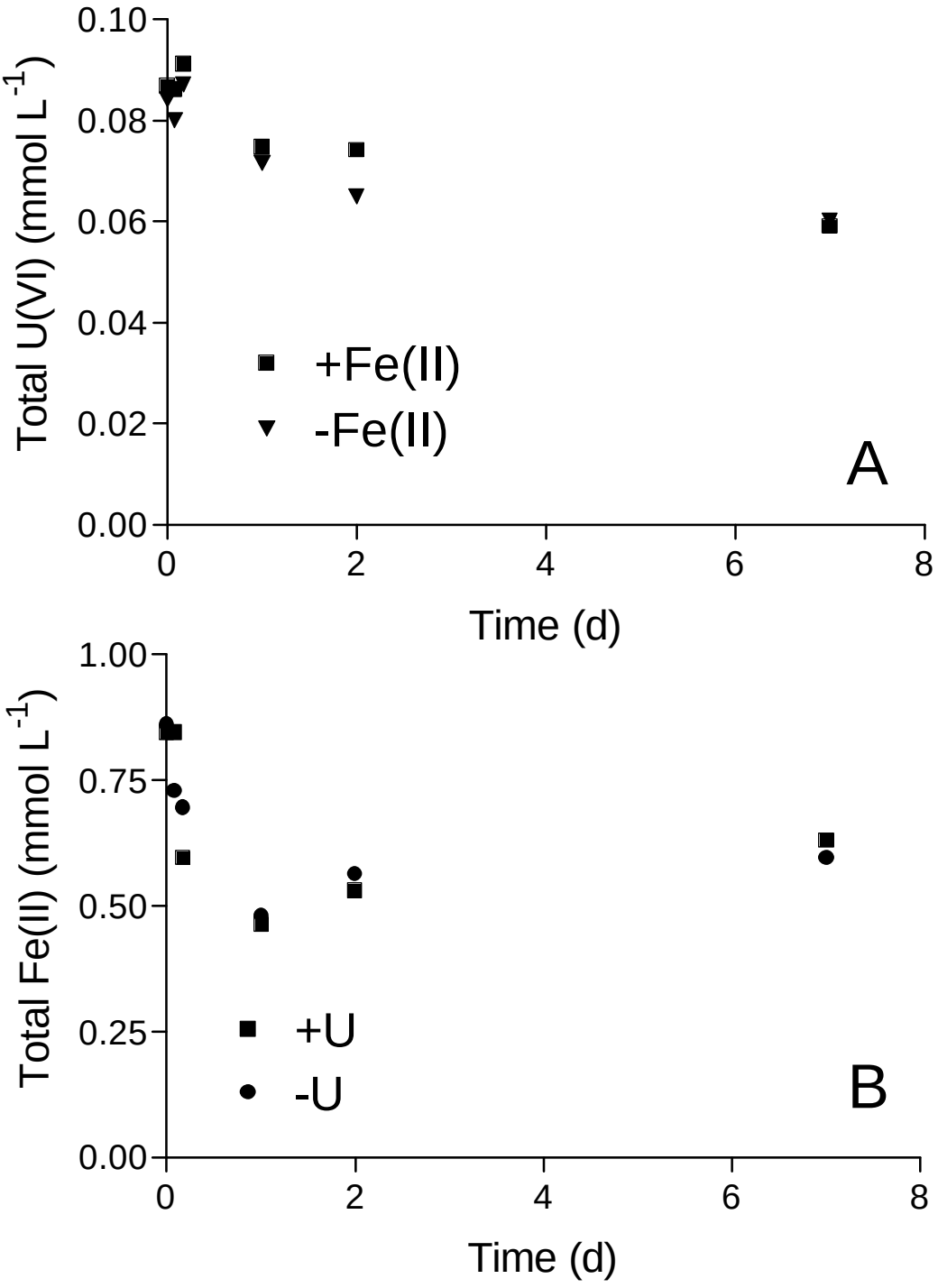

Figure 10. Reduction of U(VI) in APS-containing anaerobic PGAGW in the presence and absence of 1 mM Fe(II) (added as $FeCl_2$-$2H_2O$).

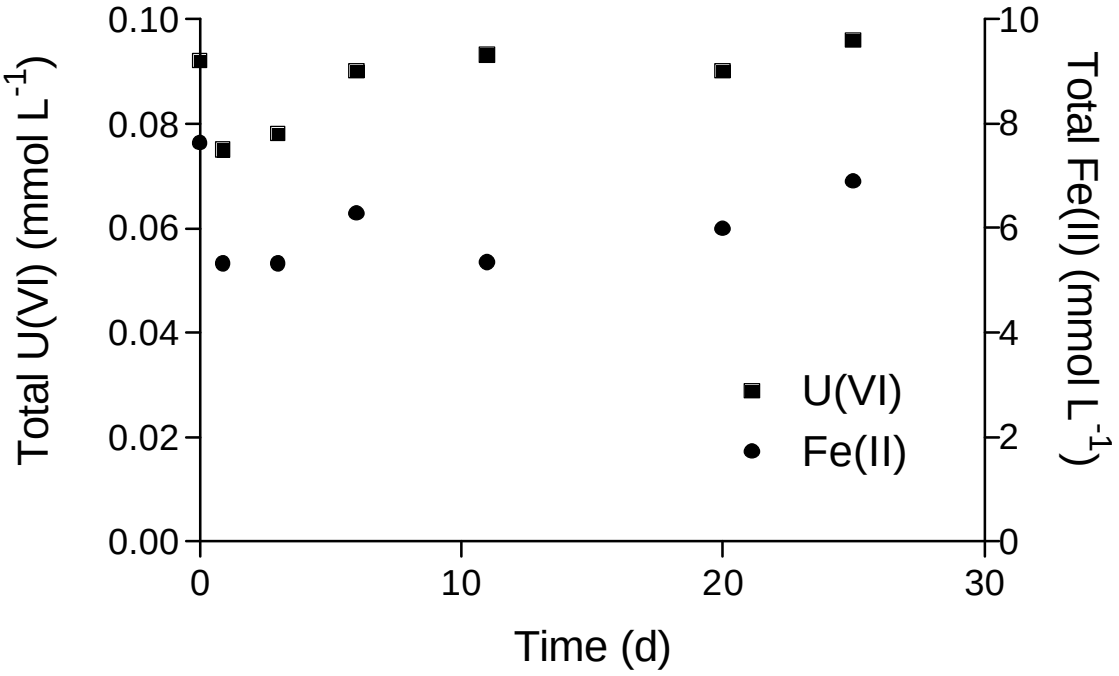

Figure 11. Abiotic reduction of U(VI) by pasteurized microbially-reduced APS (50 mmol Fe(III) L^{-1}). Data points represent means of triplicate subsamples from 100-mL culture bottles.

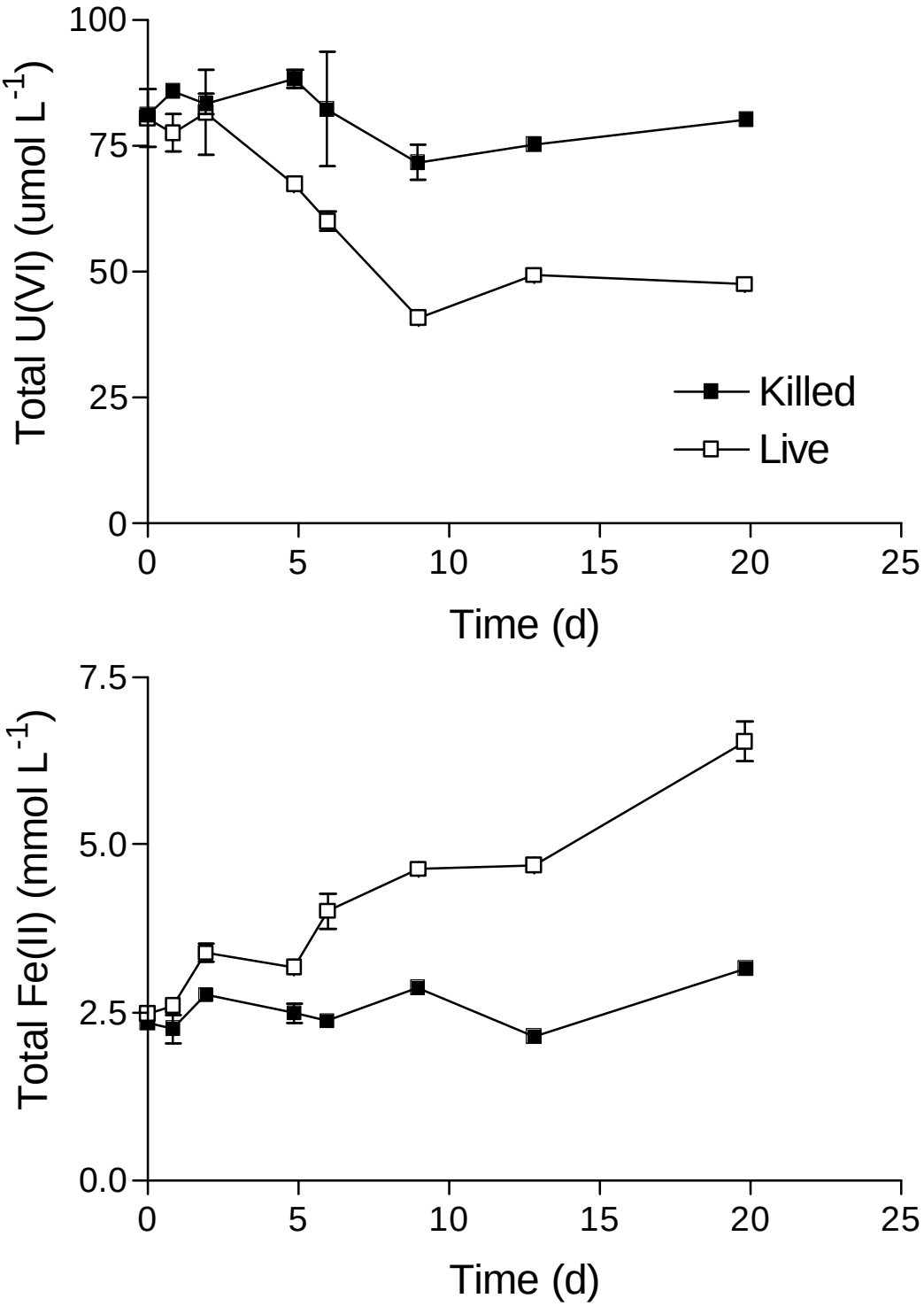

Figure 12. Reduction of U(VI) in Fe(II)-rich live vs. killed (pasteurized after 5 days of initial DMRB activity) APS reduction cultures (10^8 cells mL^{-1} of acetate/fumarate-grown *G. sulfurreducens* cells). Data points show the mean ± SD of triplicate subsamples from 100-mL reactors.

References

Barnett, M.O., P.M. Jardine, and S.C. Brooks. 2002. U(VI) adsorption to heterogeneous subsurface media: application of a surface complexation model. Environ. Sci. Technol. 36:937-942.

Caccavo, F., D.J. Lonergan, D.R. Lovley, M. Davis, J.F. Stolz, and M.J. McInerney. 1994. *Geobacter sulfurreducens* sp. nov., a hydrogen- and acetate-oxidizing dissimilatory metal-reducing microorganism. Appl. Environ. Microbiol. 60:3752-3759.

Casas, I., D. Casabona, L. Duro, and J. Depablo. 1994. The influence of hematite on the sorption of uranium(VI) onto granite filling fractures. Chem. Geol. 113:319-326.

DeFlaun, M.F., S.R. Oppenheimer, S. Streger, C.W. Condee, and M. Fletcher. 1999. Alterations in adhesion, transport, and membrane characterisitics in an adhesion-deficient Pseudomonad. Appl. Environ. Microbiol. 65:759-765.

Finneran, K.T., R.T. Anderson, K.P. Nevin, and D.R. Lovley. 2002. Potentail for bioremediation of uranium-contaminated aquifers with microbial U(VI) reduction. Soil Sed. Contamin. 11:339-357.

Fredrickson, J.K., J.M. Zachara, D.W. Kennedy, H. Dong, T.C. Onstott, N.W. Hinman, and S. Li. 1999. Biogenic iron mineralization accompanying the dissimilatory reduction of hydrous ferric oxide by a groundwater bacterium. Geochim. Cosmochim. Acta 62:3239-3257.

Fredrickson, J.K., J.M. Zachara, D.W. Kennedy, M.C. Duff, Y.A. Gorby, S.W. Li, and K.M. Krupka. 2000. Reduction of U(VI) in goethite (α-FeOOH) suspensions by a dissimilatory metal-reducing bacterium. Geochim. Cosmochim. Acta 64:3085-3098.

Gorby, Y.A., and D.R. Lovley. 1992. Enzymatic uranium precipitation. Environ. Sci. Technol. 26:205-207.

Holmes, D.E., K.T. Finneran, R.A. O'Neil, and D.R. Lovley. 2002. Enrichment of members of the family *Geobacteraceae* associated with the stimulation of dissimilatory metal reduction in uranium-contaminated aquifer sediments. Appl. Environ. Microbiol. 68:2300-2306.

Hsi, C.-K.D., and D. Langmuir. 1985. Adsorption of uranyl onto ferric oxyhydroxides: Application of the surface complexation site-binding model. Geochim. Cosmochim. Acta 49:1931-1941.

Kohler, M., G.P. Curtis, D.B. Kent, and J.A. Davis. 1996. Experimental investigation and modeling of U(VI) transport under variable chemical conditions. Wat. Resour. Res. 32:3539-3551.

Liger, E., L. Charlet, and P. VanCapellen. 1999. Surface catalysis of uranium(VI) reduction by Fe(II). Geochim. Cosmochim. Acta 63:2939-2955.

Liu, C., Y.A. Gorby, J.M. Zachara, J.K. Fredrickson, and C.F. Brown. 2002. Reduction kinetics of Fe(III), Co(III), U(VI), Cr(VI), Tc(VII) in cultures of dissimilatory metal reducing bacteria. Biotechnol. Bioengin. In press.

Lovley, D.R. 1995. Bioremediation of organic and metal contaminants with dissimilatory metal reduction. Journal of Industrial Microbiology 14:85-93.

Lovley, D.R. 2000. Fe(III) and Mn(IV) reduction, pp. 3-30. *In* Environmental metal-microbe interactions, Lovley, D.R. [ed], ASM Press.

Lovley, D.R., and E.J.P. Phillips. 1988. Novel mode of microbial energy metabolism: organic carbon oxidation coupled to dissimilatory reduction of iron or manganese. Appl. Environ. Microbiol. 54:1472-1480.

Lovley, D.R., and E.J.P. Phillips. 1992. Bioremediation of uranium contamination with enzymatic uranium reduction. Environ. Sci. Technol. 26:2228-2234.

Lovley, D.R., E.J.P. Phillips, Y.A. Gorby, and E.R. Landa. 1991. Microbial reduction of uranium. Nature 350:413-416.

Lovley, D.R., J.D. Coates, E.L. Blunt-Harris, E.J.P. Phillips, and J.C. Woodward. 1996. Humic substances as electron acceptors for microbial respiration. Nature 382:445-448.

Lovley, D.R., J.L. Fraga, E.L. Blunt-Harris, L.A. Hayes, E.J.P. Phillips, and J.D. Coates. 1998. Humic substances as a mediator for microbially catalyzed metal reduction. Acta Hydrochim. Hydrobiol. 26:152-157.

Morrison, S.J., R.R. Spangler, and V.S. Tripathi. 1995. Adsorption of uranium(VI) on amorphous ferric oxyhydroxide at high concentrations of dissolved carbon (IV) and sulfur(VI). J. Contam. Hydrol. 17:333-346.

Roden, E.E. 2002. Heterogeneity of Fe(III) oxide reactivity toward biotic vs. abiotic reduction. Environ. Sci. Technol. Submitted for publication.

Roden, E.E., and J.M. Zachara. 1996. Microbial reduction of crystalline iron(III) oxides: Influence of oxide surface area and potential for cell growth. Environ. Sci. Technol. 30:1618-1628.

Roden, E.E., and M.M. Urrutia. 1999. Ferrous iron removal promotes microbial reduction of crystalline iron(III) oxides. Environ. Sci. Technol. 33:1847-1853.

Roden, E.E., and M.M. Urrutia. 2002. Influence of biogenic Fe(II) on bacterial reduction of crystalline Fe(III) oxides. Geomicrobiol. J. 19:209-251.

Roden, E.E., and T.D. Scheibe. 2002. Multiple pore region model of uranium(VI) reductive immobilization in structured subsurface media. *In* American Geophysical Union Annual Fall Meeting. San Francisco.

Roden, E.E., M.M. Urrutia, and C.J. Mann. 2000. Bacterial reductive dissolution of crystalline Fe(III) oxide in continuous-flow column reactors. Appl. Environ. Microbiol. 66:1062-1065.

Senko, J.M., J.D. Istok, J.M. Suflita, and L.R. Krumholz. 2002. In-situ evidence for uranium immobilization and remobilization. Environ. Sci. Technol. 36:1491-1496.

Snoeyenbos-West, O.L., K.P. Nevin, R.T. Anderson, and D.R. Lovley. 2000. Enrichment of *Geobacter* species in response to stimulation of Fe(III) reduction in sandy aquifer sediments. Microb. Ecol. 39:153-167.

Ticknor, K.V. 1994. Uranium sorption on geological materials. Radiochim. Acta 64:229-236.

Truex, M.J., B.M. Peyton, N.B. Valentine, and Y.A. Gorby. 1997. Kinetics of U(VI) reduction by a dissimilatory Fe(III)-reducing bacterium under non-growth conditions. Biotech. Bioengin. 55:490-496.

Waite, T.D., J.A. Davis, T.E. Payne, G.A. Waychunas, and N. Xu. 1994. Uranium(VI) adsorption to ferrihydrite: Application of a surface complexation model. Geochim. Cosmochim. Acta 58:5465-5478.

Watson, D.B. (2002). U.S. DOE, Natural and Accelerated Bioremediation (NABIR) Program, Field Research Center Web Site. http://www.esd.ornl.gov/nabirfrc/

Wielinga, B., M.M. Mizuba, C.M. Hansel, and S. Fendorf. 2001. Iron promoted reduction of chromate by dissimilatory iron-reducing bacteria. Environ. Sci. Technol. 35:522-527.

Wielinga, B., B. Bostick, C.M. Hansel, R.F. Rosenzweig, and S. Fendorf. 2000. Inhibition of bacterially promoted uranium reduction: ferric (hydr)oxides as competitive electron acceptors. Environ. Sci. Technol. 34:2190-2195.

Zachara, J.M., C.C. Ainsworth, C.E. Cowan, and C.T. Resch. 1989. Adsorption of chromate by subsurface soil horizons. Soil Sci. Soc. Am. J. 53:418-428.

Appendix 1. Kinetic model of bacterial Fe(III) oxide reduction in subsurface sediments

Model Formulation

A kinetic model of bacterial Fe(III) oxide reduction in subsurface sediments was developed based on the results of batch Fe(III) oxide reduction experiments conducted with Abbott's Pitt Sand (APS) and *Geobacter sulfurreducens.* The model depicts enzymatic reduction of "free" Fe(III) oxide surface sites as a function of DMRB cell abundance according to a Monod-style hyperbolic kinetic function. The hyperbolic kinetic function accurately described the relationship between initial Fe(III) oxide reduction rate and *G. sulfurreducens* cell abundance (Fig. A1). The initial abundance of free oxide surface sites is defined by the molar concentration of Fe(III) oxide per dm^3 bulk volume, an assumed Fe(III) oxide molecular weight of 89 g mol^{-1}, a user-defined Fe(III) oxide specific surface area (m^2g^{-1}), and the standard value of 3.84 μmol sites per m^2 mineral surface recommended by Davis and Kent (1990). Oxide surface area is treated as an adjustable parameter in the model, the value of which value defines the maximum abundance of free surface sites per mol (or mass) of Fe(III) oxide in the system. The abundance of free surface sites declines over time due to sorption of biogenic Fe(II) onto residual Fe(III) oxide surface sites (Roden and Urrutia, 1999). This formulation provides an adequate macroscopic depiction of the impact of solid-phase Fe(II) accumulation on Fe(III) oxide reduction (Roden and Urrutia, 1999; Liu et al., 2001; Burgos et al., 2002). The sorption of Fe(II) to residual Fe(III) oxide surface sites was modeled according to a kinetically-controlled Freundlich sorption isotherm. The Freundlich isotherm parameters were obtained from data on solid-phase vs. aqueous Fe(II) accumulation during APS reduction by *G. sulfurreducens* (Fig. A2). The rate constant for Fe(II) sorption to APS were estimated from kinetic sorption studies conducted in PBAGW medium (Fig. A3). Growth of *G. sulfurreducens* biomass coupled to Fe(III) oxide reduction was assumed to occur according to yield coefficients determined previously for growth of *G. metallireducens* coupled to reduction of soluble Fe(III)-citrate (Fig. A4).

Based on the above model formulations, the following kinetic expressions depict the time course of Fe(III) oxide reduction in batch APS reduction systems:

$$\frac{d[Fe(III)]}{dt} = -R_{max}\frac{[Cells]}{K_{1/2}+[Cells]}[Fe(III)_{fss}] \qquad (A1)$$

$$\frac{d[Fe(II)_{aq}]}{dt} = -\frac{d[Fe(III)]}{dt} - k_{ads}\left([Fe(II)_{aq}] - \left(\frac{[Fe(II)_{ads}]}{K_f}\right)^{(1/n)}\right) \qquad (A2)$$

$$\frac{d[Fe(II)_{ads}]}{dt} = k_{ads}\left([Fe(II)_{aq}] - \left(\frac{[Fe(II)_{ads}]}{K_f}\right)^{(1/n)}\right) \qquad (A3)$$

$$\frac{d[Cells]}{dt} = Y\frac{d[Fe(III)]}{dt} - k_d[Cells] \qquad (A4)$$

where:

R_{max} = maximum site-specific rate of Fe(III) oxide reduction (mmol L^{-1} d^{-1}) (Fig. A1)

$K_{1/2}$ = half saturation constant for dependence of site-specific Fe(III) oxide reduction rate on DMRB cell density (mg dm^{-3}) (Fig. A1)

$[Fe(III)]_{fss}$ = concentration of "free" oxide surface sites (mmol L^{-1}) , computed as follows:

$$[Fe(III)]_{fss} = [Fe(III)] \times MW \times SA \times SSD - [Fe(II)_{ads}] \qquad (A5)$$

where $[Fe(III)]$ = bulk Fe(III) oxide concentration (mmol L^{-1})
MW = molecular weight of Fe(III) oxide ($\equiv$ 0.089 g $mmol^{-1}$)
SA = surface area of Fe(III) oxide (m^2g^{-1})
SSD = surface site density ($\equiv$ 0.00384 mmol sites m^{-2})
$[Fe(II)]_{ads}$ = bulk concentration of sorbed Fe(II) (mmol L^{-1})

K_f = Freundlich sorption parameter (Fig. A2)

n = Freundlich sorption parameter (Fig. A2)

k_{ads} = rate constant for Fe(II) sorption (d^{-1}) (Fig. A3)

Y = Yield coefficient for DMRB growth coupled to Fe(III) oxide reduction (mg mmol Fe^{-1}) (Fig. A4)

k_d = death rate constant ($\equiv$ 0.024 d^{-1}; from Tebes-Stevens et al. (1998))

Simulation Results

To initiate a simulation, the starting concentrations of Fe(III), total Fe(II), and DMRB cell density are specified, and equations A1-A4 are then integrated numerically using a fifth-order Runge-Kutta algorithm with error control (Press et al., 1992). Relative and absolute error tolerances of 0.1 % and 0.001 mmol L^{-1} were employed. For the simulations shown here, initial values of Fe(III) and total Fe(II) were set equal to 40.0 and 0.0 mmol L^{-1}, respectively, consistent with the starting conditions in the relevant APS reduction experiments.

The results of a simulation in which the initial DMRB biomass was set equal to 20 mg dm^{-3} to model an APS reduction experiment with a starting *G. sulfurreducens* cell density of ca. 10^8 cells mL^{-1} is shown in Fig. A5. This simulation was used to determine an appropriate value for Fe(III) oxide surface area (SA in equation A5). A value of 350 m^2g^{-1} yielded a total initial "free" surface site density of ca. 5 mmol L^{-1}, consistent with the total amount of Fe(II) produced during reduction of 40 mmol Fe(III) L^{-1} in the form of the APS material. Using this value for SA, the model accurately reproduced the rate and extent of APS reduction, as well as aqueous vs. solid-phase Fe(II) speciation during Fe(III) oxide reduction (Fig. A5). DMRB biomass increased only slightly during the 30-d simulation, given the high initial cell density and the relatively small amount of Fe(III) available to sustain DMRB cell growth (i.e. compared to the initial density of cells).

In order to independently evaluate the ability of the model to reproduce the results of other APS reduction experiments in which substantial growth of DMRB biomass is likely to have occurred, additional

simulations were conducted with the initial DMRB biomass set equal to either 2.0, 0.2, or 0.02 to model APS reduction experiments with initial *G. sulfurreducens* densities of ca. 10^5, 10^6, or 10^7 cells mL^{-1}, respectively. The results (Fig. A6) indicate that the model did a reasonable job of reproducing the experimental results, in particular the relatively slow rate of Fe(III) oxide reduction, and the lower overall extent of reduction in experiments with low initial DMRB densities (Fig. A6B,C). Although the predicted extent of reduction at the end of the last two simulations was ca. 2-fold higher than observed values, in general the agreement between the experimental and model results is good and suggests that the simulation framework developed here may be appropriate for use in modeling bacterial Fe(III) oxide reduction in subsurface environments. Moreover, the results suggest that this framework will be useful for simulating DMRB growth and activity in the reactive transport experiments to be conducted during Phase II and Phase III of this research project.

An important implication of the modeling results is that substantial numbers of DMRB cells (10^7-10^8 cells mL^{-1}) are likely to be produced during stimulated (e.g. via injection of soluble electron donors such as acetate or ethanol) reduction of natural Fe(III) oxides present at concentrations of 10-100 mmol per dm^3 bulk sediment – values which are typical of many Fe-rich subsurface sediments (Roden et al., 2002; Roden and Urrutia, 2002). This is an important consideration with regard to the ability of DMRB to efficiently reduce aqueous (as well as sorbed) U(VI) within biogenic redox barriers (Roden and Scheibe, 2002).

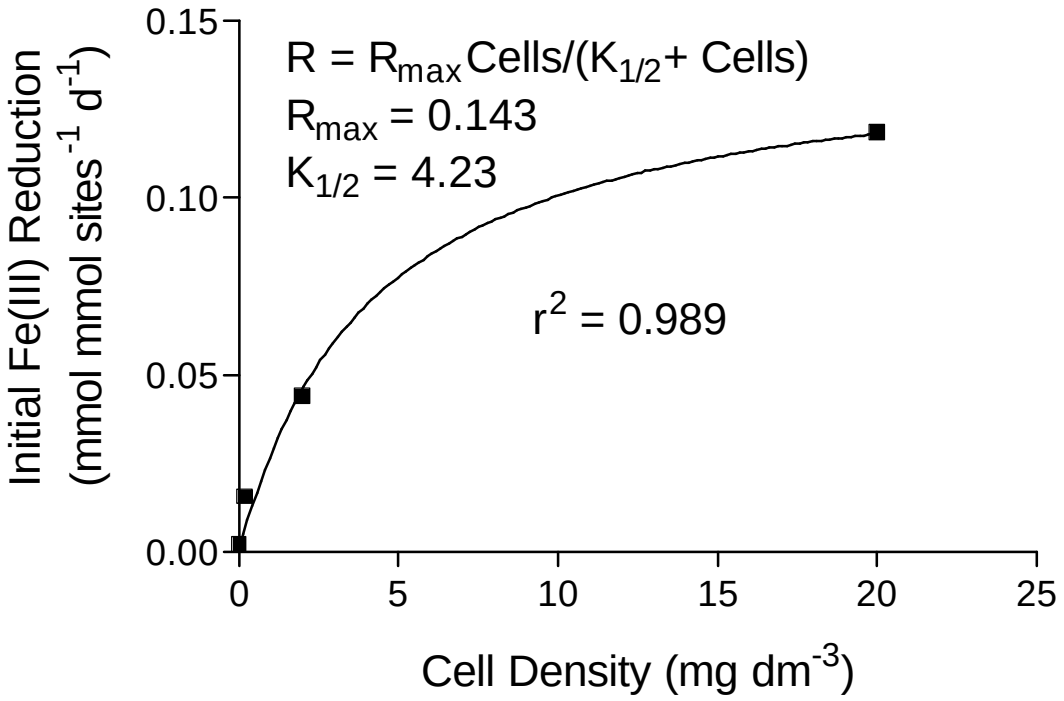

Figure A1. Initial rate of APS Fe(III) oxide reduction (initial [Fe(III)] = 40 mmol L^{-1}) by *G. sulfurreducens* under nongrowth conditions as a function of cell density. Data points represent the means of duplicate cultures. The initial density of oxide surface sites assumed in the calculation of reaction rates is defined by Eqn. A5 with SA = 350 m^2 g^{-1} (see text), and initial $[Fe(II)_{ads}]$ = 0. The line shows a nonlinear least-squares regression fit of the data to a hyperbolic kinetic function. A cell density of 20 mg dm^{-3} corresponds to ca. 10^8 cells mL^{-1}.

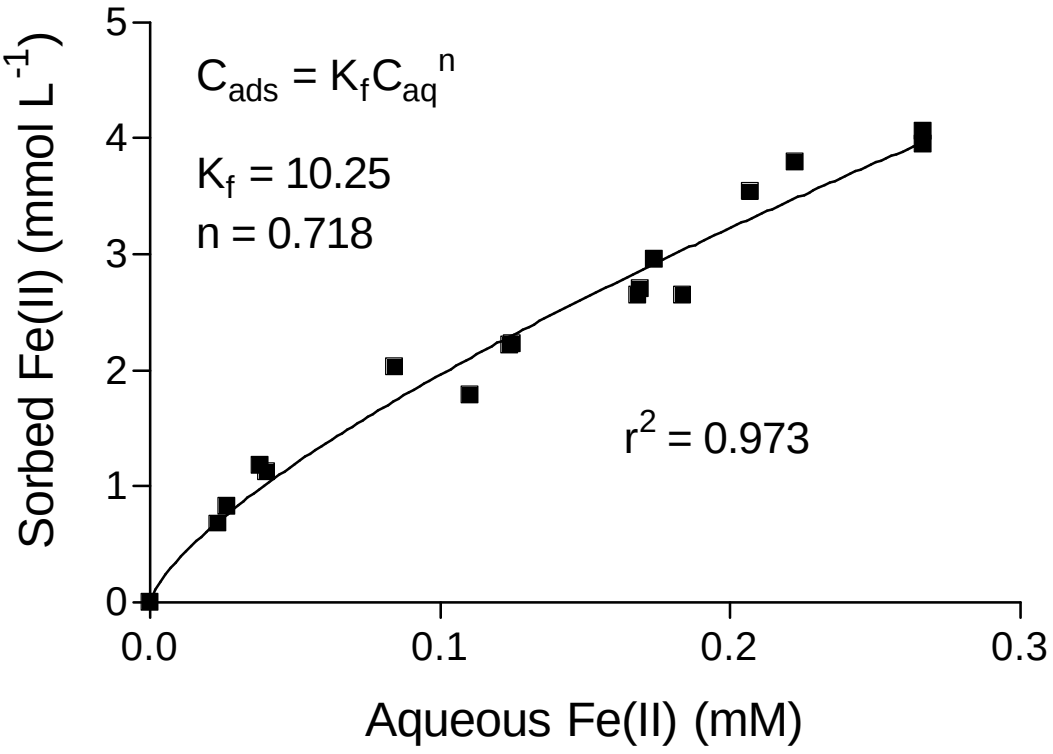

Figure A2. Accumulation of sorbed vs. aqueous Fe(II) during reduction of APS (initial Fe(III) = 40 mmol L^{-1}) by 10^8 cell mL^{-1} *G. sulfurreducens.* The line shows a nonlinear least-squares regression fit of the data to a Freundlich sorption isotherm.

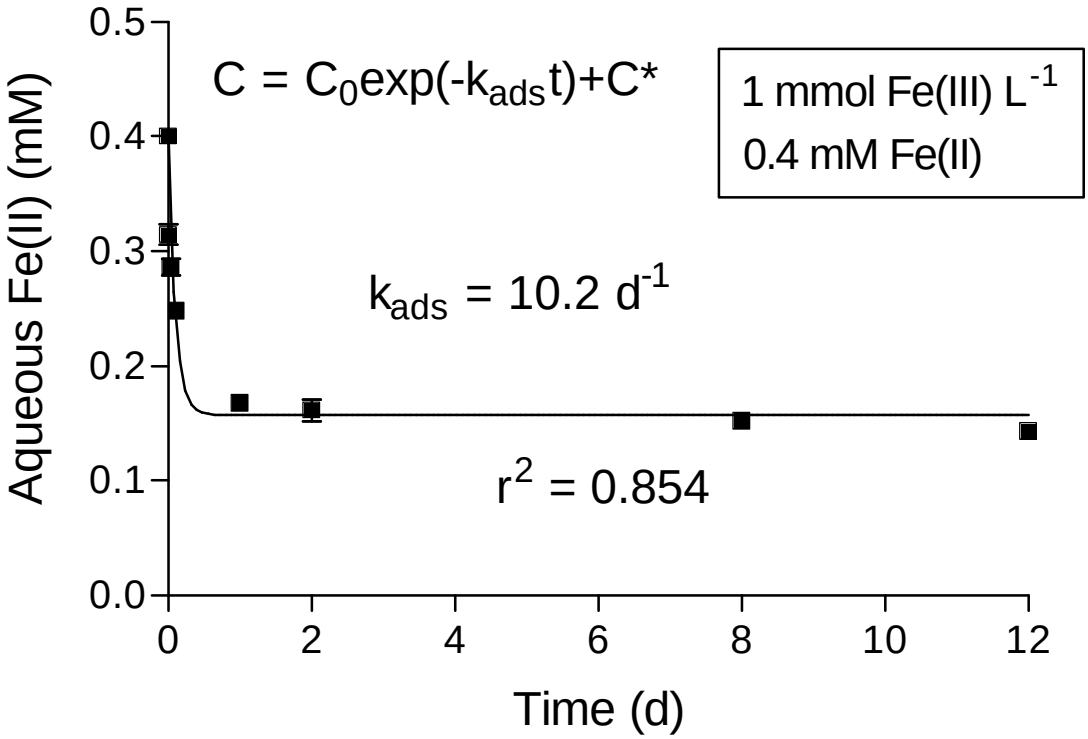

Figure A3. Kinetics of Fe(II) sorption onto APS material. Initial Fe(III) = 1 mmol L^{-1}; initial Fe(II) = 0.4 mM. Data points represent the means of triplicates. The line represents a nonlinear least-squares regression fit to an exponential decay equation.

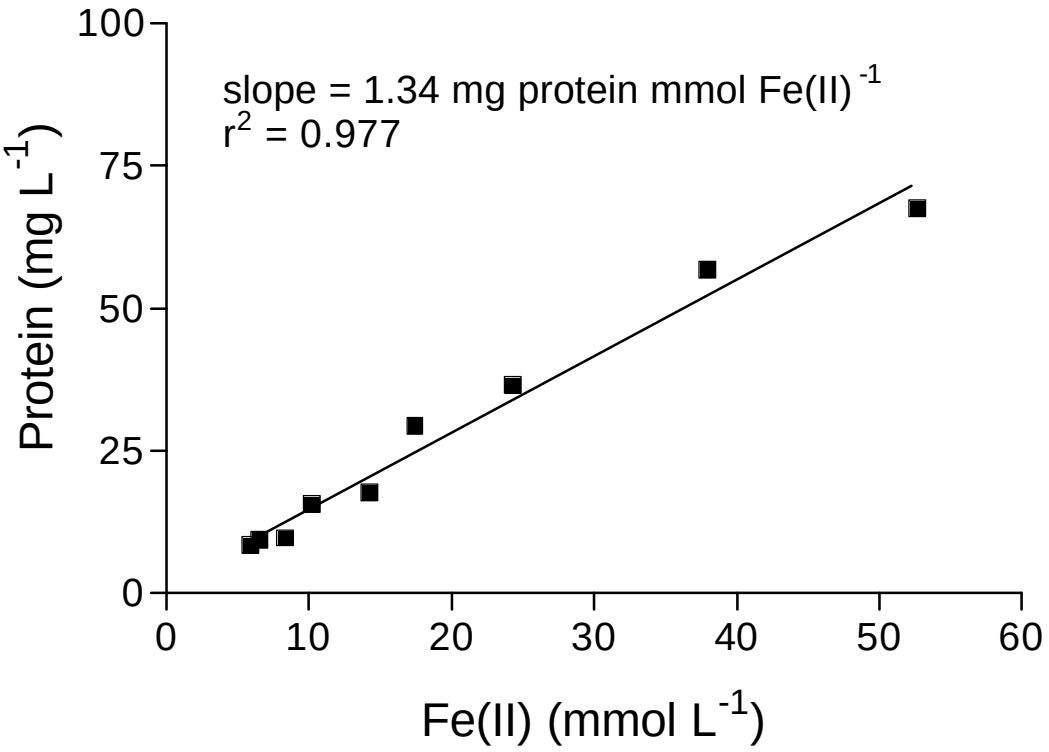

Figure A4. Growth yield of *G. metallireducens* on acetate and ferric citrate. Data points represent the means of triplicate cultures. The line shows a linear least-squares regression fit of the data.

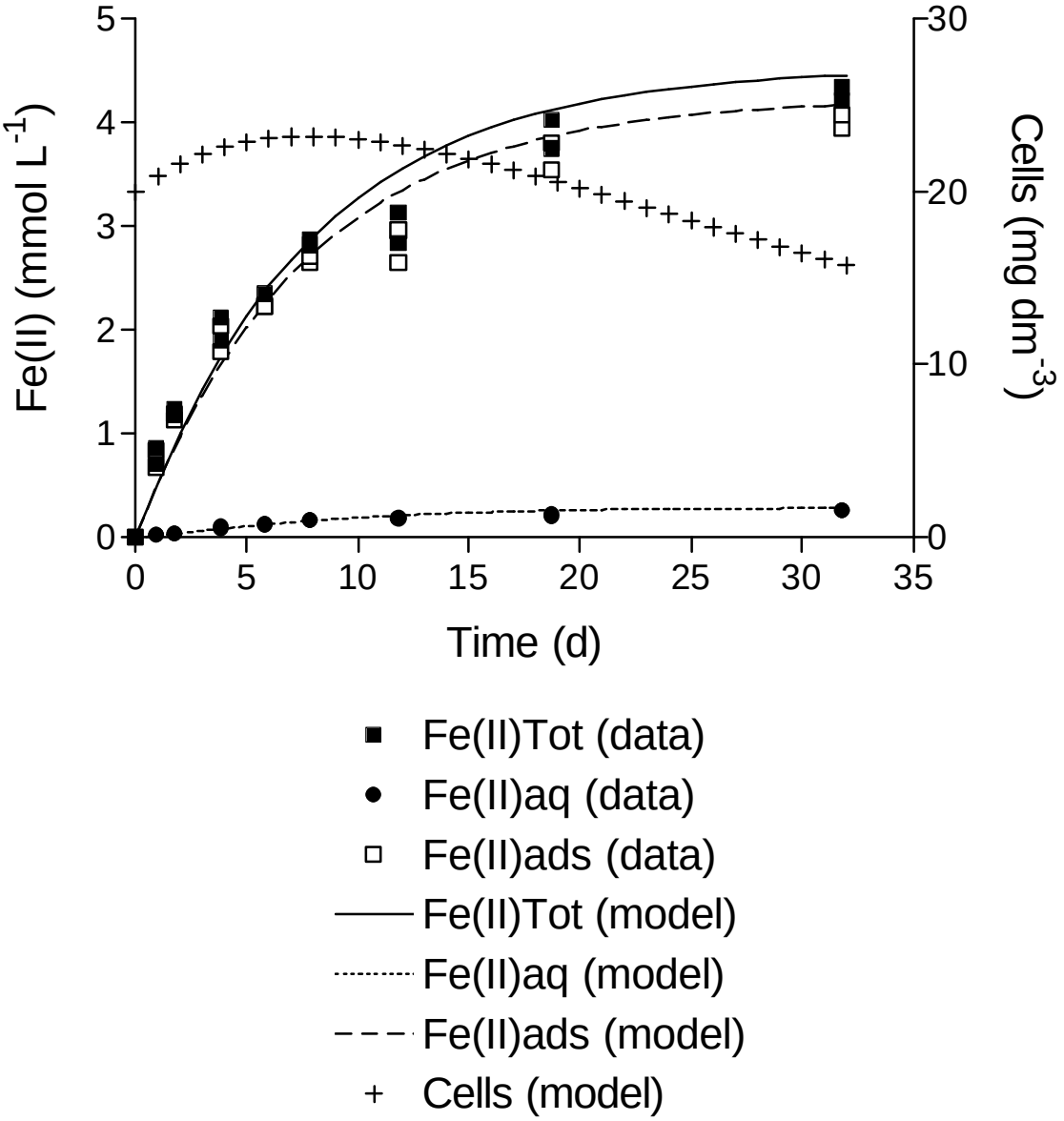

Figure A5. Simulation of APS reduction (initial Fe(III) = 40 mmol L^{-1}) with an initial DMRB biomass of 20 mg dm^{-3}. A value of 350 m^2 g^{-1} (determined by trial and error to achieve a reasonable fit to the experimental data) was used for Fe(III) oxide specific surface area (SA in equation A5).

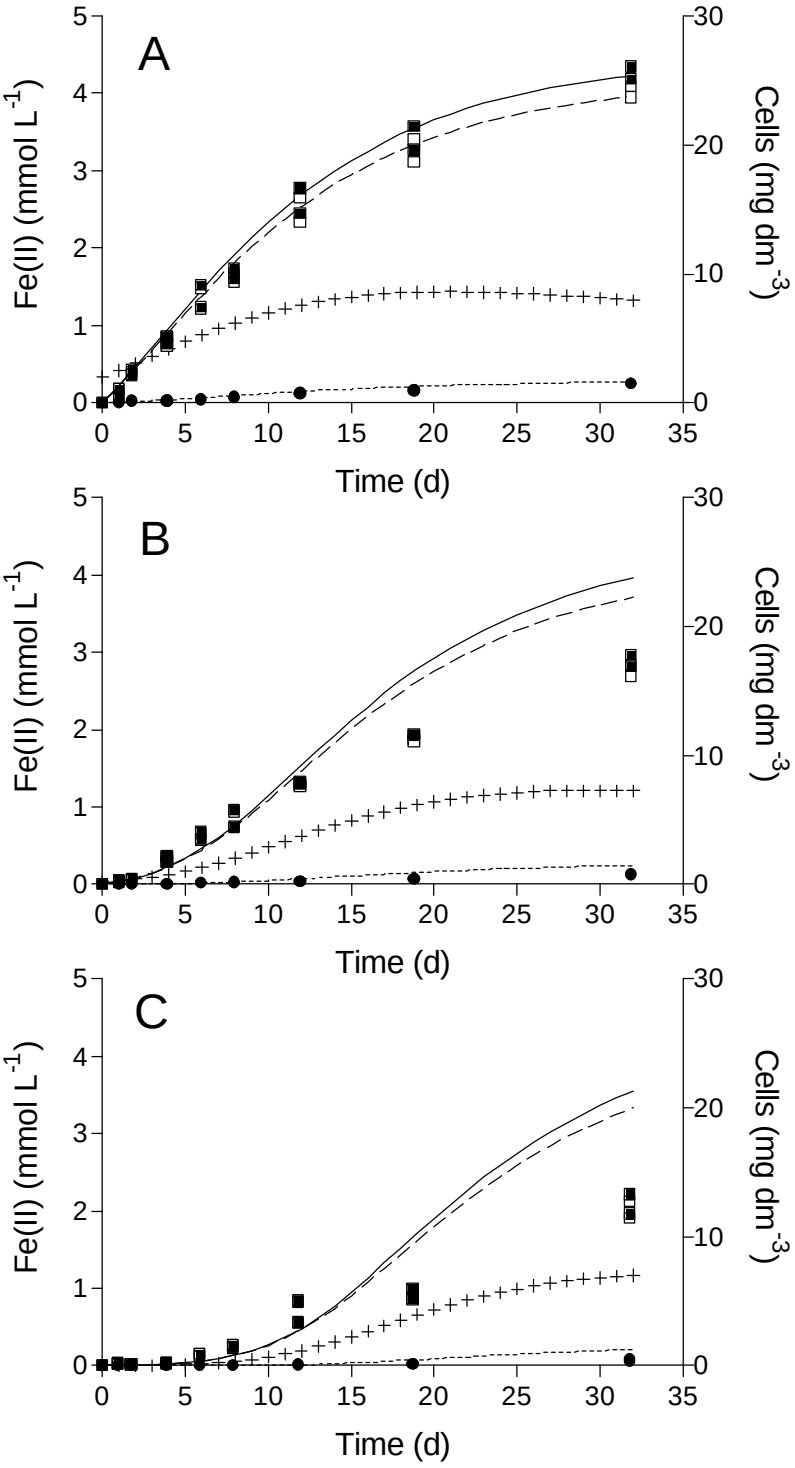

Figure A6. Simulation of APS reduction (initial Fe(III) = 40 mmol L^{-1}) with an initial DMRB biomass of 2.0 (A), 0.2 (B), or 0.02 (C) mg dm^{-3}. A value of 350 m^2 g^{-1} was used for Fe(III) oxide specific surface area in each of the simulations, based on the results of the simulation shown in Fig. A5. Symbols are the same as in Fig. A5.

References

Burgos, W.D., R.A. Royer, Y. Fang, G.T. Yeh, A.S. Fisher, B.H. Jeon, and B.A. Dempsey. 2002. Theoretical and experimental considerations related to reaction-based modeling: a case study using iron(III) oxide bioreduction. Geomicrobiol. J. 19:253-292.

Davis, J.A., and D.B. Kent. 1990. Surface complexation modeling in aqueous geochemistry, pp. 177-260. *In* Mineral-water interface geochemistry, Hochella, M.F., and A.F. White [eds], Mineralogical Society of America.

Liu, C., S. Kota, J.M. Zachara, J.K. Fredrickson, and C. Brinkman. 2001. Kinetic analysis of the bacterial reduction of goethite. Environ. Sci. Technol. 35:2482-2490.

Press, W.H., S.A. Teukolsky, W.T. Vetterling, and B.P. Flannery. 1992. Numerical Recipes in FORTRAN, Cambridge University Press.

Roden, E.E., and M.M. Urrutia. 1999. Ferrous iron removal promotes microbial reduction of crystalline iron(III) oxides. Environ. Sci. Technol. 33:1847-1853.

Roden, E.E., and M.M. Urrutia. 2002. Influence of biogenic Fe(II) on bacterial reduction of crystalline Fe(III) oxides. Geomicrobiol. J. 19:209-251.

Roden, E.E., and T.D. Scheibe. 2002. Conceptual and numerical model of uranium(VI) reductive immobilization in fractured subsurface sediments. Environ. Sci. Technol. Submitted for publication.

Roden, E.E., M.R. Leonardo, and F.G. Ferris. 2002. Immobilization of strontium during iron biomineralization coupled to dissimilatory hydrous ferric oxide reduction. Geochim. Cosmochim. Acta 66:2823-2839.

Tebes-Stevens, C., A.J. Valocchi, J.M. VanBriesen, and B.E. Rittman. 1998. Multicomponent transport with coupled geochemical and microbiological reactions: model description and example simulations. J. Hydrol. 209:8-26.